Small Photon Entangling Quantum System for Space Based Quantum Experiments

Rakhitha Chandrasekara, Zhongkan Tan, Yue Chuan Tan, Cliff Cheng and Alexander Ling
Centre for Quantum Technologies, National University of Singapore
S 15, 3 Science Drive 2, Singapore 117543; +65 6516 6897
rakhitha@nus.edu.sg

ABSTRACT

To overcome the challenges of establishing a global Quantum Key Distribution network using optical fibers, several communication protocols using satellites have been proposed. A major milestone towards such a goal is the demonstration of a working source of entangled photons on a satellite. We are building a compact instrument capable of generating entangled photon pairs through spontaneous parametric down conversion. We intend to follow an iterative development cycle with the first mission to demonstrate that the control electronics can reliably operate an optical source of correlated photons in orbit. The instrument we are building is designed to be integrated into a nanosatellite and conforms to the size, weight and power requirements of a 1U CubeSat. The instrument contains a power stabilized optical pump, single photon detectors and inertial free polarization rotators to measure polarization correlations onboard the nanosatellite. The single photon detection unit utilizes a software based controlling mechanism to achieve temperature independent operation in a typical low earth orbit nanosatellite. The integrated system has been tested for thermal, vacuum and vibration environments. The latest test on a high altitude balloon demonstrates the technology readiness of the electronics payload for space missions.

INTRODUCTION

Quantum Key Distribution (QKD) is spurred by the privacy guarantees from quantum mechanics. A number of proposals[1,2] have been been published for building global QKD networks using satellites that host quantum light sources or detectors. The most secure form of QKD relies on correlations known as entanglement[3]. The demonstration of a source of entangled photons in orbit would be a major breakthrough, enabling entanglement-assisted QKD experiments for a variety of scenarios (satellite-to-ground or inter-satellite).

Together with collaborators[4,5] we have proposed that nanosatellites are a cost-effective pathway to reach space with quantum sources onboard. They could act as demonstrators to raise the technology readiness level of essential components and also as the final platforms that transmit and receive single photons from ground-based stations or other satellites. In particular, we propose that nanosatellites can effectively host robust and compact sources of polarization-entangled photon pairs, which are the workhorse for entanglement based quantum communication. We intend to implement a series of iterative nanosatellite missions with increased scope for each step, until a final demonstration of entanglement based QKD is achieved. The decreasing cost of launching a nanosatellite into low earth orbit (LEO) has added impetus to this approach [6].

We are building a nanosatellite compatible polarization entangled photon source to be operated LEO which we call the Small Photon Entangling Quantum System (SPEQS). The optical source is based on Spontaneous Parametric Down Conversion (SPDC)[7]. An SPDC source source of photons consists primarily of a pump laser and various crystals in line with the pump light and aligned to within 0.04 degrees of accuracy. In the SPDC process, a single pump photon is sometimes converted into a pair of daughter photons obeying energy and momentum conservation. The daughter photons carry quantum correlations used in a large number of quantum communication strategies. The daughter photons are identified from coincident detection of photons at two separate single photon detectors.

For characterization of the SPDC source and the polarization correlations that are produced detectors and polarization rotators are necessary. Thus, the electronics platform for the SPEQS instrument must operate a number of opto-electronic devices efficiently. These include the diode laser for the pump beam, the Geiger-mode avalanche photodiodes (GM-APD) for detecting single photons and polarization rotators.

In addition to the operation of the opto-electronic devices, the SPEQS instrument must store experiment

data before transferring it to a satellite on board computer (OBC). Experiment data are primarily in the form of photo-detection events generated by the GM-APDs, and associated house-keeping data such as laser power and temperature.

For our first mission, we intend to demonstrate that the control electronics is capable of operating a single photon source. For this mission, we intend to implement the electronics platform and integrated it with a correlated photon source (a correlated photon source is simply an unoptimized entangled photon source). The simplified optics enables the collected data to be interpreted with greater clarity and enables a stronger statement to be made on the suitability of the control electronics platform for the more advanced missions that will be flown in the future.

In this paper we discuss the implementation of the electronics platform and focus on the key subsystems that are contained within it. A full description of the optical system and its build process is being prepared. We will present also the results of the various qualification tests and conclude with a discussion of our program road-map that is true at the time of submission.

ELECTRONICS SUBSYSTEMS

A full description of the electronics platform is available elsewhere[8]. Our intention here is to briefly remind the reader of the more important circuits that are needed to operate a single photon source. The electronics platform is designed around the Cypress CY8C3666 Programmable-System-On-Chip (PSoC3) micro-controller. The PSoC3 is an 8-bit, 8051 architecture bundled together with configurable analog and digital blocks such as counters, timers, analogue-to-digital converters (ADC), digital-to-analogue converters (DAC) and pulse-width-modulation (PWM). The advantage of a PSoC type device is that a large number of the analog and digital blocks are commonly used in optical detection and control circuits, so this reduces the use of discrete integrated chips, greatly simplifying the board layout.

Figure 1 illustrates the main subsystems integrated into SPEQS instrument to conduct the quantum experiment. We will describe the GM-APD controller and polarization rotator in some detail.

The SPEQS instrument can be operated on 5V supply from a satellite bus via standard PC-104 connector as shown in Figure 1. The system is capable of regulating voltage at 3.3V (logic), 9V and 12V for other opto-electronic systems. A Commercial DC to DC step up converters generate 9V and 12V. The thermal management sub system maintains the temperature of the optical unit above a target temperature (above which the optical experiment is able to work reliably).

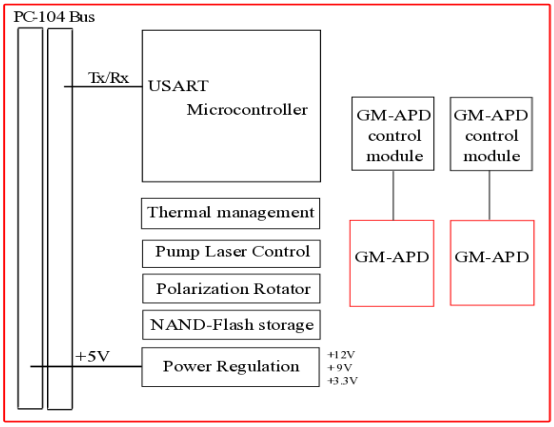

Figure 1: Payload subsystems for SPEQS. All the subsystems are controlled by the micro-controller. The controllers for the GM-APD, Pump Laser and Thermal Management run in closed loops while the Polarization Rotator is an open loop system.

Photon pairs generated by the SPDC process are detected by a pair of GM-APDs. The photon detection efficiency of GM-APDs depends on the excess of bias voltage over the (temperature dependent) breakdown voltage. In the case of fixed bias voltage operation (as commonly implemented), the excess voltage decreases with increasing temperature. In fact, even if the case temperature were constant, a high rate of photons would increase the GM-APD junction temperature resulting in a lower detection efficiency. This is widely known and accepted as a limitation of GM-APDs[9].

We have overcome this problem of temperature dependent detection efficiency using a software based feedback mechanism[10]. The basic idea is illustrated in Figure 2. A reversed biased GM-APD registers a pulse after a constant level discriminator (CLD) if the pulse height is higher than the threshold voltage ($V_{r,t}$). A single avalanche pulse is split in to two pulses (top and bottom) with different pulse heights as determined by the resistor ladder. We define top (to CLD1) and bottom (to CLD2) pulses in the diagram. By setting different threshold levels for CLDs ($V_{r,t}$ and $V_{r,b}$) we can detect a predefined percentage of top pulses at CLD2 at a given temperature and bias voltage (V_a). This ratio is a function of temperature present on GM-APD. A real time ratio monitoring allows the system to adjust V_a to maintain a predefined ratio. This achieves stable detection efficiency that is independent of temperature and yet does not rely directly on temperature sensors.

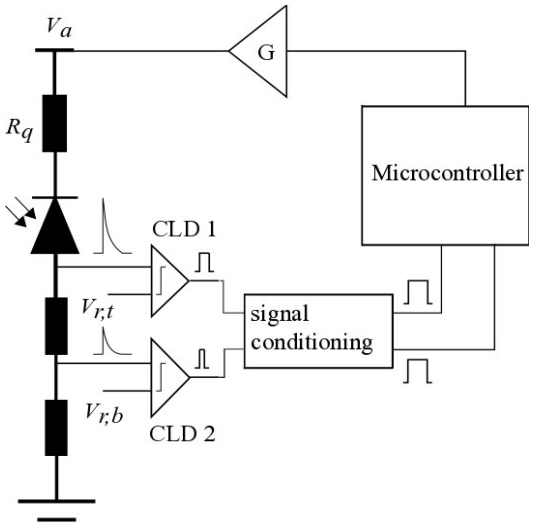

Figure 2: The window comparator implementation for GM-APDs. A single photo-detection event is split into two current pulses. By comparing the ratio of pulse heights, we evaluate whether the photon detection efficiency is within a desired range.

The source quality is defined in terms of the rate of observed coincident detection between detectors, and also the quality of the relative polarization contrast between the down converted photons. Implementation of coincidence detection is straightforward. The coincidence detection circuit uses an AND gate picks up the temporal overlap of photon detection pulses from each GM-APD.

To minimize the rate of accidental collisions between unrelated pulses, the duration of each pulse is kept at 4.3ns. This leads to an overall coincidence window of 8.6 ns. A shorter window is possible, but only at the expense of more power consumption due to the need for faster logic devices. The minimum and maximum coincidences are used to quantify the quality (visibility) of the single photon source.

In order to obtain a variation in the correlations, however, the photons must be passed through a rotating polarization filter. In a laboratory experiment this is commonly achieved with motor based polarizers. Motors, however, introduce torque. For use onboard small satellites, however, inertial free polarization rotators are required to mitigate any interference with the satellite attitude control system. In addition, motors are heavy, power intensive and have other problems associated with vacuum operation.

In SPEQS we use nematic liquid crystal based polarization rotators (LCPR) placed in front of fixed polarizing filters. The position of the LCPRs can be seen in Figure 5. The degree of polarization rotation experienced by an incoming photon is a function of the (AC) voltage amplitude applied to the LCPR.

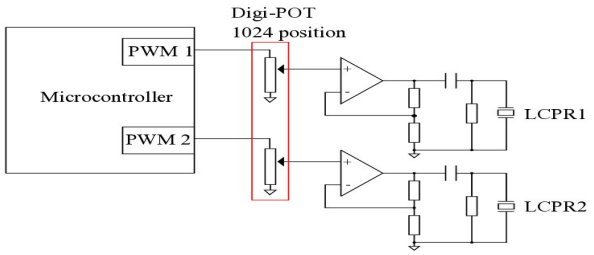

Figure 3: The polarization rotator controller generates an AC square wave using PsoC3 in-built pulse width modulators (PWM) along with an external digital potentiometer (Digi-POT). The amplitude of the PWM signal is controlled using the Digi-POT taper position. After achieving the required amplification it goes through a high pass filter to generate the AC signal.

Figure 3 illustrates the implementation of the open loop electronic controller which generates the required AC signal. Figure 4 illustrates the change in coincidences (correlations) between two detectors as the LCPR (LCD) voltage is changed. In an actual experimental run, the LCPRs experience a voltage ramp and for each value of the ramp, GM-APDs are accumulated. This enables the brightness and quality of the polarization correlations to be quantified.

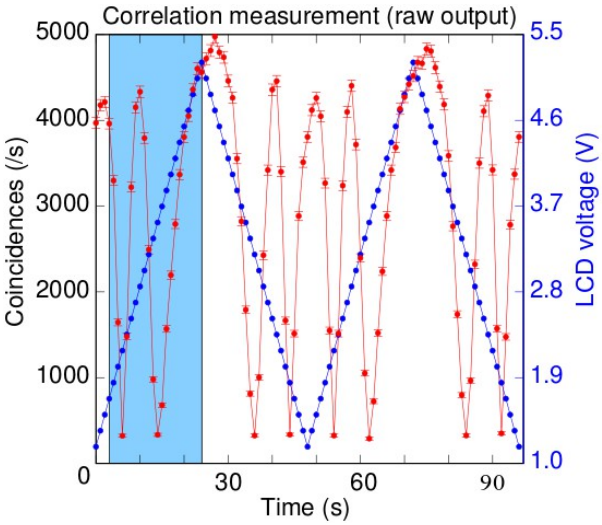

Figure 4: The coincidences (correlations) between two detectors per second depends on the polarization filter settings in front of the detector. The red graph indicates the variation in the observed correlations. The visibility is not unity because of accidental correlations. For a basic correlated source as in this experiment, we expect unit visibility after deduction of the accidental correlations that arise from the finite width of the detection pulses. The LCPRs implemented in SPEQS can achieve 2π rotation.

OPTICAL SUBSYSTEM

The optical set up consists of two sections, source and the detection. The source section is capable of accommodating a laser diode, 5 different bi-refringent crystals necessary for the production of entangled photons, and the necessary optics for preparing the pump beam and for its removal. The source section also holds a P-I-N photodiode used for monitoring and stabilization of pump power.

In the detection section, there is room to house four GM-APDs. By using polarizing beam splitter (PBS) cubes as the polarization filters, there is the option for using four detectors in total to achieve detector redundancy. In front of each PBS cube is a LCPR for the necessary polarization rotation. The layout of crystals and detectors is illustrated in Figure 5.

The entire optical unit is integrated with the electronics platform that acts as the mechanical interface to the CubeSat. Optical components are secured to the optical tray using two component epoxy that has good outgassing properties. Currently, the design has no space for optical lenses; consequently, the overall optical instrument suffers from a low detection efficiency (about 2%). However, the signal-to-noise ratio is still sufficient for a high confidence demonstration of quantum entanglement. Originally, the optical design was made to accommodate four detectors. Detectors 2 and 3 (see Figure 5) were designated as back-up detectors that were turned on only when necessary as they suffered from optical cross-talk (during each photo-detection event, a GM-APD would give off a flash of light). Further testing, however, led to increased confidence in the survivability of the GM-APD segments and in the interest of weight savings, the backup detectors have been removed from the latest instrument models.

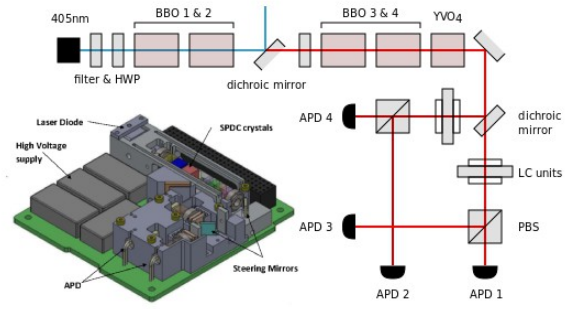

Figure 5: Optical set up of the SPEQS instrument. The control electronics are on the reverse side of the FR4-based printed circuit board (green). Entangled photons are generated in beta Barium Borate crystals (BBO1&2). The additional crystals BBO3&4 and YVO4 are used to optimize the correlations between photon pairs and to achieve entanglement. For the first mission, however, only BBO1 will be present as that is sufficient to test the control electronics.

QUALIFICATION TESTS

A large number of components that have been identified for used in the SPEQS instrument are available as commercial-off-the-shelf items, with no space heritage. In order to gain confidence that these components would work in the final copy, a test campaign covering radiation, thermal, vacuum and vibration environments was conducted. These tests culminated in a test at near-space using a balloon. The tests were also conducted with the unoptimized photon source and so the optical unit contained only a single BBO crystal.

Radiation test results have been reported elsewhere[11], and we only describe the highlights of the findings here. The most radiation sensitive components (as expected from literature) were the GM-APDs (SAP500) that appeared to perform as excellent dosimeters for deposited energy. Despite this sensitivity, analysis of radiation profiles in LEO strongly suggests that GM-APDs embedded with CubeSats should remain operational during the orbital life of the CubeSat. Other opto-electronic components have so far shown very promising insensitivity to test dosage and suggests good in-orbit performance.

The integrated electronics platform was also exposed to radiation and only the memory storage devices demonstrated sensitivity. Entire sectors of the flash memory device (M25P80 SPI Flash) were wiped out and replaced with a repeating bit pattern that can be used as evidence of memory loss. A simple mitigation strategy of writing data to multiple physical sectors could overcome this effect.

Figure 6: The complete electronics platform being prepared for exposure to proton flux at the Crocker Nuclear Laboratory, UC Davis.

Apart from radiation tests, the SPEQS instrument (a single copy) has been tested for thermal, vacuum and vibration profiles in order to qualify it for space missions. The test profiles are readily available from a number of launch providers and from literature. The protocol for each test was the same: a baseline performance was collected prior to the test, and after the test a comparison of the performance was made.

The SPEQS instrument was powered off during each test. The baseline visibility recorded for the copy was 93% ± 2% and did not change over the test campaign. The next set of graphs show SPEQS performance after each of test.

Vacuum Test

The main concern for vacuum testing is to check the outgassing of materials (eg: epoxy, FR-4) at low pressures which could change the transmission properties of crystals. The vacuum test was conducted at 10^{-6} mbar over 24 hours. Figure 7 shows the post test results.

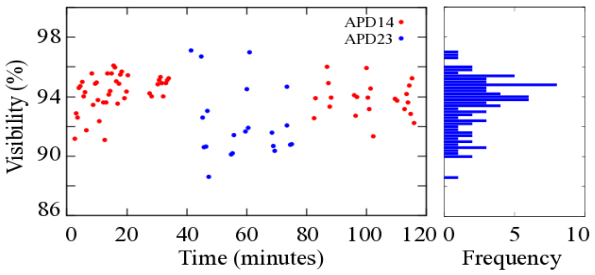

Figure 7: After the vacuum test the SPEQS instrument visibility was maintained at 94 ± 1%.

Thermal Cycling

The thermal cycling test was conducted to check the thermal fatigue of the SPEQS instrument. Each temperature cycle consists of a temperature ramp from -10 ^{0}C to 40 ^{0}C (50 minutes) followed by a ramp back to -10 ^{0}C (50 minutes) over 24 hours. Figure 8 shows the test results after thermal cycling. In addition, an actual qualification model was thermally soaked at 45 ^{0}C and -20 ^{0}C for six hours at each temperature and after the test, the SPEQS instrument still produced a visibility of 93%.

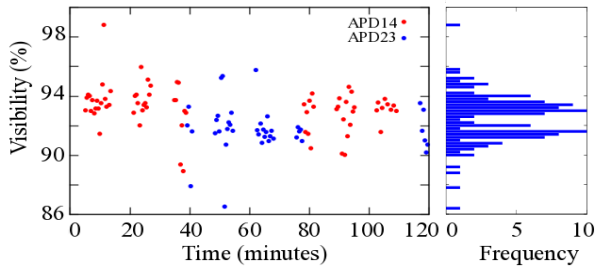

Figure 8: The visibility of the SPEQS instrument after thermal cycling maintained at 93 ± 2% .

Vibration Test

The SPEQS instrument was tested for vibration according to the specifications set by the Cyclone-4 launcher[12]. Most launch vehicles available to the small satellite community have similar or more forgiving conditions. The vibration test profiles consist of sine sweep and random vibration test for all three axes. Table 1 shows the values used for each test.

Table 1: Vibration test profiles

Description \Test type	Sine sweep	Random Vibration
X – axis	0.5 g, 2.5g	7.4 g (rms)
Y – axis	0.5 g, 2.5g	7.4 g (rms)
Z – axis	0.5 g, 2.5 g	7.4 g (rms)
Frequency (Hz)	5-10 Hz, 10-100 Hz	20-2000 Hz

Figure 9 shows the post vibration test results after z axis test. Here the z axis is defined on the face of the payload.

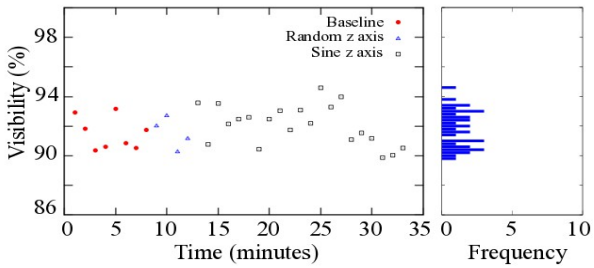

Figure 9: Vibration test results for SPEQS in z direction. The average visibility after testing for 3 axes was 92 ± 2 %.

Near Space Experiment

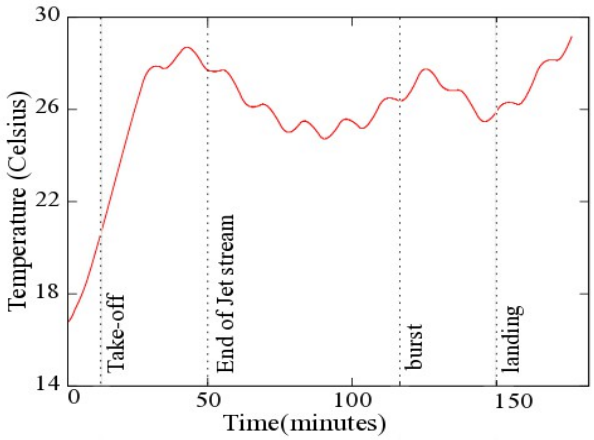

Figure 10: During flight the SPEQS instrument experienced temperature variations from 17 ^{0}C to 30 ^{0}C. Initial temperature gradient of ~0.5 ^{0}C/min is typical to polar orbit nanosatellites. The temperature of the SPEQS instrument is determined from two thermistors placed at two ends of the device.

The integrated package was tested in a weather balloon which lofted up to 35.5km altitude[13]. This near-space

test flight provided the opportunity to test the integrated instrument in a very realistic environment where temperature and vibration was not under control and where pressure was essentially vacuum.

The temperature gradient experienced by the SPEQS instrument is ~0.5 ^{0}C/min which is comparable with typical polar orbit temperatures[14]. Figure 10 shows the temperature experienced by the SPEQS instrument during the flight. The performance of the laser diode system is shown in Figure 11. The temperature of the laser diode also changed from 17 ^{0}C to 30 ^{0}C during the flight and the power remained relatively steady within a 0.25 mW range over the entire flight. This was corroborated by observing the steady state rate of photons impinging on one of the GM-APDs which recorded an average rate of 360,000 detection events per second irrespective of temperature. The detector data, in turn, is taken as evidence that the photon detection efficiency was steady throughout the flight.

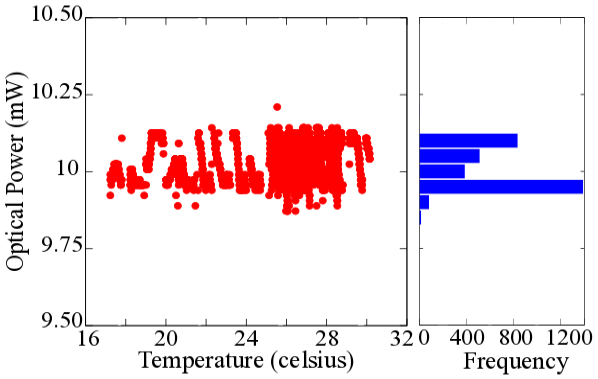

Figure 11: The feedback system managed to maintain 10.029 ± 0.068 mW of optical power independent of the temperature.

DISCUSSION

The various tests strongly suggest that the implementation of the electronics platform will be able to support photon counting experiments on board nanosatellites. The current implementation of the source consumes approximately 1.4 W of power during normal operation, while having an approximate mass of 250 gm. The current implementation follows strictly the CubeSat specifications and is available to nanosatellite teams for integration into their spacecraft upon request.

Since 2014, the instrument has undergone two launch campaigns. The first launch campaign was with the Danish GomX-2 spacecraft that was unfortunately lost in a launch vehicle failure in October 2014. However, the experience gained from that particular campaign has increased the confidence level for SPEQS operation in low Earth orbit.

A second launch campaign is currently underway with the NUS Galassia satellite[14]. This satellite is due for launch on the Polar Space Launch Vehicle (India) in late 2015 with experimental data expected in the first quarter of 2016. Successful experimental data will enable the first milestone on our proposed QKD program using small satellites.

We note, however, that the GomX-2 and Galassia missions would have covered very different orbital parameters. GomX-2 was supposed to have been in an ISS compatible orbit, while Galassia is nearly equatorial. Two sets of data would have been enabled a comprehensive comparison of the performance of the two copies in orbit to understand if the orbital environment has a significant impact on the control electronics. This would be important input for future missions where choice of orbit is often restricted to polar or ISS-compatible orbits due to the presence of optical ground receivers being primarily present in the Northern hemisphere.

We point out, however, that our instrument is designed strictly to the CubeSat standard and is available for other small satellite developers who wish to collaborate on the development of quantum technology for space. We invite interested colleagues to get in touch with us.

From the experience of the SPEQS team, the choice to adopt the CubeSat standard has been quite fruitful. By maintaining a comprehensive Interface Control Document and a straightforward Concept of Operations, our team has managed to support two very different satellite groups.

The team is now working on the next iteration of the SPEQS instruments, where a full-entangled source will be operated within the form-factor we have presented in this document. A test and verification campaign is currently being planned, and we expect to repeat the same cycle of testing by the end of 2015. We are also evaluating the utility of sounding rockets as a proving ground for qualification testing.

It should also be noted, however, that the current form-factor is rather restrictive and compromises the brightness of the optical source. To include longer crystals and collection lenses for pump and downconverted photons, we are confident of detecting photons at the rate of several million per second (in contrast to the current rate of several thousand). In order for this to be implemented, however, a dedidcated spacecraft is required. We are currently preparing the designs for this next generation instrument (designated as SPEQS-2.0) and the supporting spacecraft (designated as SpooQy-Sat).

Acknowledgments

During the development of this platform, C. Cheng and Tan Y. C. were supported by the DSO-CQT project on quantum sensors. Both of them are currently supported by the National Research Foundation project NRF-CRP12-2013- 02. James Grieve and Robert Bedington assisted with graphical and text at various points of this manuscript.

REFERENCES

1. R. Ursin *et al.*, "Space-quest, experiments with quantum entanglement in space," *Europhysics News*, vol. 40, no. 3, pp. 26–29, 2009

2. T. Scheidl, E. Wille, and R. Ursin, "Quantum optics experiments using the International Space Station: a proposal," *New Journal of Physics*, vol. 15, no. 4, p. 043008, 2013.

3. A. Ekert, "Quantum cryptography based on Bell's theorem", *Physical Review Letters*, vol. 67, pp.661-663, 1991.

4. W. Morong, A. Ling, and D. Oi, "Quantum optics for space platforms," *Optics and Photonics News*, pp. 42–49, October 2012.

5. A. Ling and D. Oi, "Small Photon-Entangling Quantum Systems (SPEQS) for LEO Satellites," in *Proc. International Conference on Space Optical System and Applications (ICSOS)*, vol. 12. Ajaccio: ICSOS, 2012.

6. J. Coopersmith, "The cost of reaching orbit: Ground-based launch systems", *Space Policy,* vol. 27, no. 2, pp. 77-80, 2011

7. D. C. Burnham and D. L. Weinberg, "Observation of simultaneity in parametric production of optical photon pairs," *Phys. Rev. Lett.*, vol. 25, pp. 84–87, 1970.

8. C. Cheng, R. Chandrasekara, Tan Y. C. and A. Ling, "Space qualified nanosatellite electronics platform for photon pair experiments", arXiv:1505.06523, 2015

9. R. G. W. Brown, R. Jones, J. G. Rarity and K. D. Ridley, "Characterization of silicon avalanche photodiodes for photon correlation measurements. 2: Active quenching", *Applied Optics*, vol. 26, no. 12, pp. 2382-2389, 1987

10. R. Chandrasekara, Z.K Tang, Y.C Tan, C. Cheng , C. Wildfeuer, A. Ling, "Single photon counting for space based quantum experiments," Proc. SPIE 9492, Advanced Photon Counting Techniques IX, 949209, 2015

11. Tan Y. C., R. Chandrasekara, C. Cheng and A. Ling, "Silicon avalanche photodiode operation and lifetime analysis for small satellites", *Opt. Exp.*, vol. 21, pp. 16946-16954, 2013. Tan Y. C., R. Chandrasekara, C. Cheng and A. Ling, "Radiation tolerance of opto-electronics components proposed for space-based quantum key distribution", *J. Mod. Optics*, DOI:10.1080/09500340.2015.1046519

12. Cyclone-4 launch vehicle user's guide (2010).

13. Tang, Z., Chandrasekara, R., Sean, Y. Y., Cheng, C., Wildfeuer, C., and Ling, A., "Near-space flight of a correlated photon system," *Scientific Reports*, vol. 4, 6366, 2014

14. J. Kataoka, *et al.*, "In-orbit performance of avalanche photodiode as radiation detector on board the picosatellite cute-1.7+apid ii", *J. of Geophysical Research*, vol. 116, no. A5, A05204, 2010

15. Luo Sha, Mouthaan Koenraad, Soh Wee Seng, Goh Cher Hiang and Alexander Ling, "Galassia System and Mission", *Small Satellite Conference*, SSC14-XI-2, 2014.